

See discussions, stats, and author profiles for this publication at: <https://www.researchgate.net/publication/261137063>

ChemInform Abstract: Structure and Biological Activity of 8-Deoxyheronamide C from a Marine-Derived Streptomyces sp.: Heronamides Target Saturated Hydrocarbon Chains in Lipid Membr...

ARTICLE *in* JOURNAL OF THE AMERICAN CHEMICAL SOCIETY · MARCH 2014

Impact Factor: 12.11 · DOI: 10.1021/ja500128u · Source: PubMed

CITATIONS

8

READS

69

6 AUTHORS, INCLUDING:



Shinichi Nishimura

Kyoto University

37 PUBLICATIONS 650 CITATIONS

[SEE PROFILE](#)



Yuta Tsunematsu

University of Shizuoka

18 PUBLICATIONS 128 CITATIONS

[SEE PROFILE](#)

Structure and Biological Activity of 8-Deoxyheronamide C from a Marine-Derived *Streptomyces* sp.: Heronamides Target Saturated Hydrocarbon Chains in Lipid Membranes

Ryosuke Sugiyama,[†] Shinichi Nishimura,^{*,†} Nobuaki Matsumori,[‡] Yuta Tsunematsu,^{†,§} Akira Hattori,[†] and Hideaki Kakeya^{*,†}

[†]Department of System Chemotherapy and Molecular Sciences, Division of Bioinformatics and Chemical Genomics, Graduate School of Pharmaceutical Sciences, Kyoto University, Sakyo-ku, Kyoto 606-8501, Japan

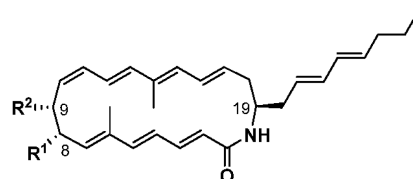
[‡]Department of Chemistry, Graduate School of Science, Osaka University, Toyonaka, Osaka 560-0043, Japan

S Supporting Information

ABSTRACT: Polyene macrolactams are a class of microbial metabolites, many of which show potent biological activities with unidentified modes of action. Here we report that 8-deoxyheronamide C, a new 20-membered polyene macrolactam from a marine-derived actinomycete *Streptomyces* sp., is a unique membrane binder. 8-Deoxyheronamide C showed a characteristic sensitivity profile against fission yeast sterol mutant cells, indicating that the metabolite targets cell membranes. We detected tight physical interaction between heronamides including 8-deoxyheronamide C and heronamide C and saturated hydrocarbon chains in lipid membranes using surface plasmon resonance experiments. We further show that heronamides induced abnormal cell wall morphology in fission yeast probably by perturbing the structure of membrane microdomains. This work will accelerate the biological and medical investigation of polyene macrolactams.

amphotericin B (AmB) and syringomycin E.^{10,11} We screened microbial culture extracts and identified a marine-derived actinomycete *Streptomyces* sp., whose culture extract showed less toxicity to the fission yeast cells lacking *erg2* gene than to wild-type cells (Figure S3). Bioassay-guided fractionation afforded 8-deoxyheronamide C (8-dHC, 1), a new 20-membered polyene macrolactam as an active constituent (Chart 1). Metabolite 1 is a putative biosynthetic precursor

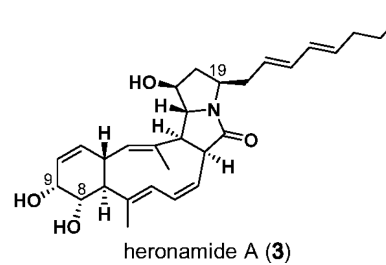
Chart 1. Chemical Structures of Heronamides



8-deoxyheronamide C (8-dHC, 1): R¹ = H, R² = OH

heronamide C (2): R¹ = R² = OH

heronamide C diacetate (4): R¹ = R² = OAc



Nature seems to have facilitated survival of living things possessing defensive mechanisms against competitive organisms; production of antibiotics is one such survival method.^{1–4} Polyene macrolactams are a class of bioactive metabolites produced by actinomycetes (Figure S1). They exhibit a variety of biological activities, including antimicrobial⁵ and antitumor activities,^{6,7} modulation of Bcl-xL function,⁸ and inhibition of leukocyte adhesion.⁹ There have been no reports, however, on the identification of their target molecules.

The cell membrane is a common target of antibiotics, and a variety of chemical classes are known to bind membrane lipids, e.g., polyene macrolides, peptides, lipopeptides, and saponins, some of which have been utilized as medicine. Small molecules that exhibit characteristic phenotypes upon binding to membrane lipids could be used as chemical tools to dissect the structure and function of cell membranes. Most antibiotics, however, quickly damage the cell membrane and are not suitable for a chemical genetics approach. To obtain novel membrane-targeting natural products, we focused on a traditional chemical genetic interaction (Figure S2); mutant yeast cells lacking ergosterol biosynthetic genes, as represented by *erg2* and *erg3*, are tolerant to lipid-binding antibiotics such as

of the polyene macrolactam heronamide C (2).¹² In fact, the microbial culture also contained 2 and heronamide A (3), both of which were originally reported from an Australian marine-derived actinomycete (Figure S4).¹²

The chemical structure of 1 was deduced by spectroscopic analysis and a chemical conversion experiment inspired by the proposed biosynthetic pathway.¹² The planar structure of 1 was determined as an 8-deoxy congener of heronamide C (2) by MS and NMR experiments (Supplementary method; Figures

Received: January 6, 2014

Published: March 26, 2014



S5 and S6; Table S1). The relative stereochemistry of **1** was deduced by interpretation of the NOESY spectrum (Figure S7). NOESY analysis was also conducted for **2**, revealing that **1** and **2** have the same relative stereochemistry at C9 and C19. This was supported by the characteristic Cotton effect in their CD spectra (Figure S7), simultaneously indicating that the absolute stereochemistry was shared between metabolites **1** and **2**. Next we investigated the biosynthetic mechanisms. A biosynthetic study of a closely related macrolactam metabolite, BE-14106 (Figure S1), revealed that the C8 hydroxyl group was introduced by cytochrome P450 monooxygenase following formation of the macrolactam ring.¹³ In fact, an 8-deoxy congener of BE-14106 has been reported.¹⁴ It is likely that **1** is a biosynthetic precursor of **2**, itself being proposed to undergo epoxidation and cyclization to afford **3** (Figure S4).¹² Based on our previous report on the stereochemistry of **3**,¹⁵ we predicted that **2** possessed a stereochemistry of 8S, 9R, 19R. Interestingly, it was discovered that **2** spontaneously converted to **3** in DMSO, confirming that the absolute stereochemistry is conserved between metabolites **2** and **3** (Figure S8). In combination, these results allowed us to conclude that the absolute configuration of **1** is 8S, 19R.

Metabolite **1** inhibited the growth of wild-type fission yeast cells with a minimum inhibitory concentration (MIC) of 5.8 μM . Growth inhibitory activities were also examined against cells mutant for ergosterol biosynthesis: cells lacking *erg2*, *erg31* and *erg32*, *erg5* or *sts1/erg4* gene (Figure S2). Interestingly, all mutant cells were tolerant to **1**; growth of mutant cells was observed even in the presence of 46 μM of the metabolite (Figure 1a). Next we examined the structure–activity relation-

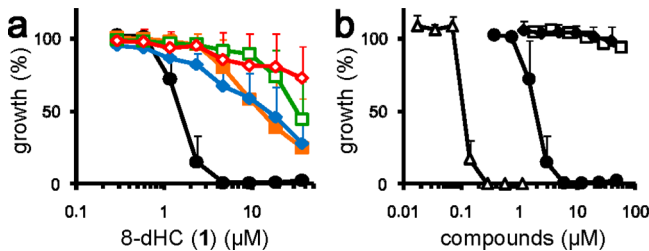


Figure 1. Sensitivity profile of heronamides to yeast sterol mutant cells. (a) Tolerance of ergosterol mutant cells to 8-dHC (**1**). Growth of wild-type (black), $\Delta\text{erg}2$ (red), $\Delta\text{erg}31$, $\Delta\text{erg}32$ (blue), $\Delta\text{sts}1/\text{erg}4$ (orange), and $\Delta\text{erg}5$ (green) cells were measured in the presence of various concentration of 8-dHC (**1**). (b) Effect of heronamides on wild-type fission yeast cells. Cells were incubated with compound **1** (circle), **2** (triangle), **3** (square), or **4** (diamond) for 24 h, and cell growth was measured. Data represent the mean of three independent experiments. Error bars indicate SD.

ship (SAR) of heronamides. Metabolite **2** exhibited more potent growth inhibitory activity (MIC, 0.28 μM) than metabolite **1**, whereas acetylated heronamide C (**4**) lost growth inhibitory activity, thus implying the importance of the hydroxyl groups (Figure 1b). Metabolite **3** exhibited no growth inhibition (Figure 1b), suggesting that the 20-membered macrolactam ring was also essential for the biological activity. Metabolite **2** showed almost no specificity; MIC values for *erg* mutants were 0.28 μM , which was identical to the activity displayed against the wild-type cells (Figure S9).

Yeast ergosterol mutants have been reported to show tolerance to membrane-targeting antibiotics such as AmB,^{10,11} indicating that metabolite **1** targets cell membrane. Mutant cells

were still sensitive to metabolite **2**, nonspecificity however does not preclude the possibility that metabolite **2** targets the cell membrane. For example, *erg* mutant cells were not tolerant to amphotericin B (**3**) that specifically recognizes membrane sterols (Figure S10).¹⁶ These results suggested that heronamides **1** and **2** might be unique membrane binders.

To investigate the affinity between heronamides and lipid membranes, we conducted surface plasmon resonance (SPR) experiments. We used a Biacore CM3 chip, in which liposomes were immobilized on dodecylamine attached via condensation through the amide bond (Supplementary methods). Using this system, we successfully detected the significantly higher affinity of AmB to 1-palmitoyl-2-oleoyl-sn-glycero-3-phosphocholine (POPC) liposomes containing 20 mol % ergosterol, compared with POPC liposomes alone (Figure S11). In analogy with sterol-targeting molecules, e.g., AmB¹⁷ and theonellamide A (TNM-A),¹⁸ we initially expected that **1** would show higher affinity to sterol-containing liposomes. Contrary to our expectations, however, this was not the case for heronamides: both **1** and **2** displayed only weak binding to POPC membranes, which were not influenced by the presence of ergosterol (Figures 2a, S12).

The type of acyl groups present in phospholipids is critical to the nature of the membrane, e.g., fluidity. For this reason we examined liposomes consisting of 1,2-dioleoyl-sn-glycero-3-phosphocholine (DOPC) or 1,2-dimyristoyl-sn-glycero-3-phosphocholine (DMPC); DOPC has two unsaturated acyl chains, whereas DMPC has two saturated ones. When DOPC liposomes containing ergosterol were immobilized on the sensor chip, only weak binding of **1** was observed, which was comparable to that of POPC membranes (Figure S12). In contrast, liposomes consisting of DMPC exhibited drastically increased binding affinity to **1**. Although the increase in the resonance unit was only several-fold, the resonance unit linearly increased during the association phase, and almost no dissociation was observed (Figure 2a). This indicated that **1** binds to the DMPC liposomes, in an irreversible manner.

Phospholipids of fission yeast contain primarily 18:1 fatty acyls.¹⁹ In contrast, the predominant type of sphingolipid was reported to be t18:0/26:0, consisting of phytosphingosine and a long saturated fatty acid. To examine the possibility that sphingolipids are targeted by **1**, we tested the binding to sphingomyelin (SM) liposomes. As expected, irreversible binding of **1** to SM liposomes was observed, and its affinity was comparable to DMPC (Figure 2a). It is worth noting that inclusion of ergosterol or cholesterol did not affect the affinity pattern of **1** toward lipid membranes (Figures S12 and S13). All experiments were conducted at 30 °C. At this temperature DMPC membranes display a liquid disordered phase, whereas DMPC membranes containing cholesterol are a mixture of liquid disordered and ordered phases. SM membranes are in a gel phase. This indicates that the membrane fluidity is unlikely to affect the affinity of **1**. Rather, **1** seems to favor lipid molecules possessing saturated hydrocarbon chains.

Heronamides exhibited growth inhibition of fission yeast cells; its potency was dependent on the number of hydroxyl groups and presence of a 20-membered macrolactam ring (Figure 1b). We subsequently investigated the SAR of heronamides in SPR experiments. Metabolite **2**, that showed growth inhibitory activity against wild-type cells 10 times more potent than the deoxy congener **1**, exhibited 8.4 times higher affinity to DMPC membranes (Figure 2b). In contrast, protection of the hydroxyl groups eliminated not only the

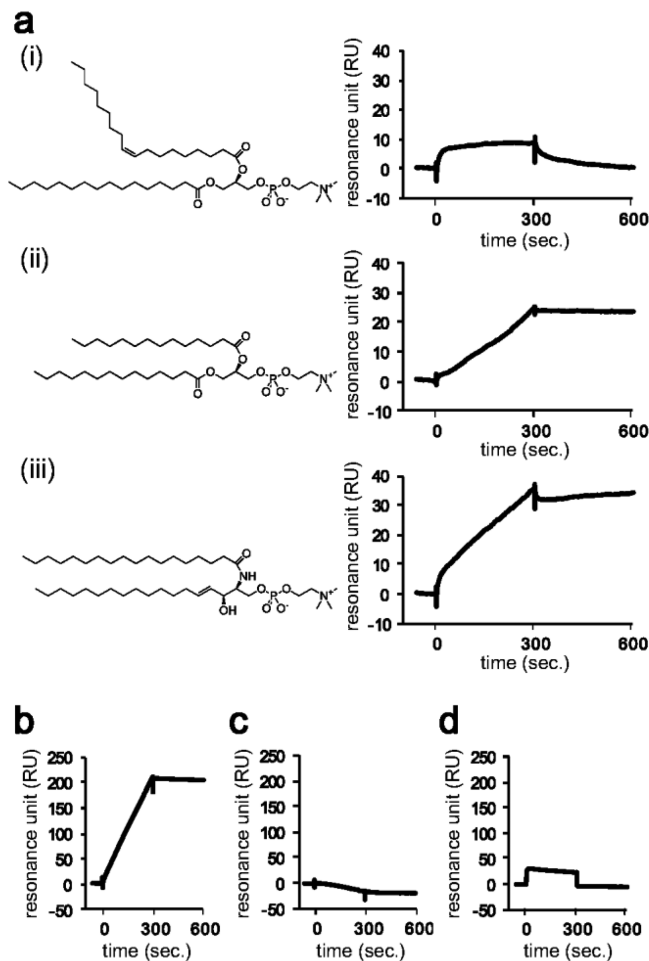


Figure 2. Affinity of heronamides to liposomes. (a) Chemical structures of the phospholipids used for the SPR experiments and sensorgrams for binding of 8-dHC (**1**) to liposomes. 20 mol % ergosterol-containing (i) POPC and (ii) DMPC liposomes and (iii) 20 mol % cholesterol-containing SM liposomes were captured on a dodecylamine-modified CM3 sensor chip. (b-d) Sensorgrams for binding of heronamides to 20 mol % ergosterol-containing DMPC liposomes. The affinity of (b) heronamide C (**2**), (c) heronamide C diacetate (**4**), and (d) heronamide A (**3**) are compared. Similar results were obtained for more than three experiments, and the characteristic sensorgrams are shown. Elution of 20 μ M heronamides was started at time 0 and maintained for 300 s. Flow rate was 10 μ L/min.

growth inhibition but also the affinity to lipid membranes (Figure 2c). In addition, metabolite 3, an inactive congener, showed a box-type sensorgram, indicating its weak and nonspecific binding to the lipid membrane (Figure 2d).

Finally, we carried out morphological analysis to investigate the consequence of heronamide binding to yeast cell membranes. We were unable to detect significant damage in bright-field images following treatment of cells with **1** or **2**. Such damage would include formation of large vacuoles, a characteristic effect of polyene antibiotics that target membrane ergosterols in yeast (Figure S14). This result supported the data obtained in the SPR experiments; response curves of heronamides were seldom affected by the inclusion of ergosterol (Figures 2, S12, and S13). Instead, metabolite-treated cells exhibited slightly abnormal septa. Detailed analysis revealed that heronamides **1** and **2** induced accumulation of cell wall material at both cell tips and septa (Figure 3a–c).

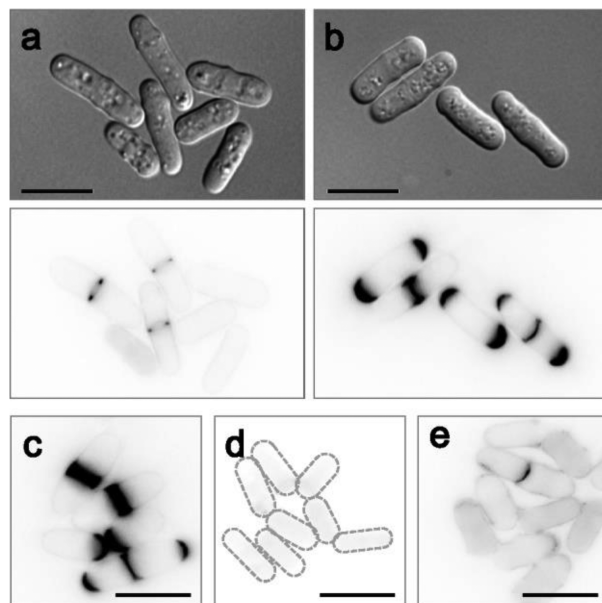


Figure 3. Cell wall abnormalities induced by heronamides. (a–c) Abnormal cell wall morphology induced by heronamides. Wild-type cells were exposed to DMSO (a, 1% v/v, solvent for compounds), 8-dHC (1) (b, 10 μ M), or heronamide C (2) (c, 1 μ M) for 2 h. (d–e) Involvement of Rho1 and Bgs1 in the action of 8-dHC (1). Cells expressing dominant-negative Rho1 protein, Rho1T20N (d) or bgs1 temperature-sensitive mutant cells with lowered glucan synthase activity (e) were treated with 8-dHC (1) (10 μ M). In all experiments, cells were fixed with formalin and stained with calcofluor white (Cfw) to visualize cell wall material. In a–b, differential interference contrast (DIC; upper) and Cfw (lower) images are shown. DIC images for (c–e) are included in Figures S15 and S16. Scale bars indicate 10 μ m.

Importantly, *css1* temperature-sensitive mutant cells are known to display similar morphological changes when placed under restriction temperature (Figure S15); *css1* gene encodes sphingolipid-phospholipase C.²⁰ It is likely that heronamides and *css1* mutation have a similar effect on the cell membrane by perturbing the function of sphingolipids. Interestingly, similar cell wall defect is induced by TNM-A (Figure S15). We have reported that TNMs induce accumulation of 1,3- β -glucan by binding to membrane ergosterol, and the phenomenon is dependent on Bgs1, a putative 1,3- β -glucan synthase catalytic subunit, and a small GTPase Rho1.²¹ This was also the case for cell wall abnormalities induced by heronamides. Neither cells expressing dominant-negative mutant Rho1 protein (Rho1T20N) nor *bgs1* mutant cells possessing low glucan synthase activity showed abnormal accumulation of cell wall material after treating cells with heronamides (Figures 3d–e, S16).

Lipid rafts are tightly packed sphingolipid and sterol-rich liquid-ordered membrane domains.²² In this study, heronamides have been revealed to favor lipid molecules with saturated hydrocarbon chains, e.g., DMPC and SM. TNMs are known to bind membrane sterols, whereas the *css1* gene product regulates sphingolipid metabolism. It is likely that cell wall biosynthesis requires functional lipid domains consisting of sphingolipids and sterols, which were perturbed by treatment with heronamides or TNMs or mutation of the *css1* gene (Figure S17). In fact, Bgs1 is a membrane protein containing 13 potential transmembrane helices and was shown to be insoluble in nonionic detergents,²³ one of the characteristics of lipid-rafts.

proteins. It is noted that heronamide treatment or *css1* mutation slowly induced accumulation of cell wall material (Figure S1S), whereas TNM-A induced a similar phenomenon quickly, suggesting that the role of sphingolipids and sterols in membrane microdomains can be distinguished using a chemical genetics approach.

Not only sphingolipid mutant but also ergosterol mutant cells become less sensitive to syringomycin E, whose channel forming activity is regulated by sphingolipids in artificial model membranes.²⁴ This suggests that modulation of sterol species affects the activity of membrane sphingolipids. This can be the cause for the tolerance of ergosterol mutant cells to 8-dHC. However, modulation of sphingolipid activity might be moderate, which is not effective enough for cells to obtain tolerance to heronamide C that has a higher affinity to lipids. Alternatively, we cannot exclude the possibility that ergosterol contributes to the action of 8-dHC in cell membranes. The role of the hydroxyl group at C8 for membrane affinity is under investigation.²⁵

In summary, we present the structures, biological activities, and membrane affinities of heronamides. Heronamides are 20-membered macrolactam metabolites. Their molecular size suggests that heronamides can act as pseudosterols. Cholesterol, e.g., has a preference for interaction with lipids that have fully saturated hydrocarbon chains when compared with lipids that have unsaturated chains.²⁶ In this context, the membrane affinity of other polyene macrolactams, whose ring size varies from 18 to 26, is of interest. Finally, introducing a hydroxyl group at C8 to 8-deoxyheronamide C (**1**) was shown to produce a highly active metabolite, suggesting the post-polyketide synthase hydroxylation enzyme responsible for the hydroxylation has proved evolutionarily favorable to the organism.

ASSOCIATED CONTENT

Supporting Information

Experimental details, structure elucidation, and biological and biophysical evaluations. This material is available free of charge via the Internet at <http://pubs.acs.org>.

AUTHOR INFORMATION

Corresponding Author

nshin@pharm.kyoto-u.ac.jp; scseigyo-hisyo@pharm.kyoto-u.ac.jp

Present Address

[§]Department of Pharmaceutical Sciences, University of Shizuoka, Shizuoka 422–8526, Japan.

Notes

The authors declare no competing financial interest.

ACKNOWLEDGMENTS

We thank Drs. S. Sato and M. Katayama (Nippon Suisan Kaisha Ltd, Japan), and Dr. H. Onaka (The University of Tokyo) for their support in the isolation and culture of the heronamide-producing strain. We are grateful to Dr. K. Takegawa (Kyushu University) for *erg* deletion strains, Dr. K. Nakano (University of Tsukuba) for *rhol* expression plasmids, Dr. T. Kuno for the *bgs1* mutant strain, and Dr. K. L. Gould (Vanderbilt University School of Medicine) for the *css1* mutant strain. We also thank Drs. M. Murata and R. A. Espiritu (Osaka University) for a kind gift of amphidinol 3, and Mr. Y. Nakagawa (Osaka University) for technical assistance of SPR

experiments. This work was supported in part by research grants from the Japan Society for the Promotion of Science, the Ministry of Education, Culture, Sports, Science, and Technology of Japan, the Ministry of Health, Labour and Welfare of Japan, and the Suntory Institute for Bioorganic Research.

REFERENCES

- Dixon, R. A. *Nature* **2001**, *411*, 843.
- Ahuja, I.; Kissin, R.; Bones, A. M. *Trends Plant Sci.* **2012**, *17*, 73.
- Rohlf, M.; Churchill, A. C. *Fungal Genet. Biol.* **2011**, *48*, 23.
- Wietz, M.; Duncan, K.; Patin, N. V.; Jensen, P. R. *J. Chem. Ecol.* **2013**, *39*, 879.
- Kojiri, K.; Nakajima, S.; Suzuki, H.; Kondo, H.; Suda, H. *J. Antibiot. (Tokyo)* **1992**, *45*, 868.
- Komiyama, K.; Iwasaki, K.; Miura, M.; Yamamoto, H.; Nozawa, Y.; Umezawa, I. *J. Antibiot. (Tokyo)* **1985**, *38*, 1614.
- Shindo, K.; Kamishohara, M.; Odagawa, A.; Matsuoka, M.; Kawai, H. *J. Antibiot. (Tokyo)* **1993**, *46*, 1076.
- Futamura, Y.; Sawa, R.; Umezawa, Y.; Igarashi, M.; Nakamura, H.; Hasegawa, K.; Yamasaki, M.; Tashiro, E.; Takahashi, Y.; Akamatsu, Y.; Imoto, M. *J. Am. Chem. Soc.* **2008**, *130*, 1822.
- Nazare, M.; Waldmann, H. *Angew. Chem., Int. Ed.* **2000**, *39*, 1125.
- Hampsey, M. *Yeast* **1997**, *13*, 1099.
- Iwaki, T.; Iefuji, H.; Hiraga, Y.; Hosomi, A.; Morita, T.; Giga-Hama, Y.; Takegawa, K. *Microbiology* **2008**, *154*, 830.
- Raju, R.; Piggott, A. M.; Conte, M. M.; Capon, R. *J. Org. Biomol. Chem.* **2010**, *8*, 4682.
- Jorgensen, H.; Degnes, K. F.; Sletta, H.; Fjaervik, E.; Dikiy, A.; Herfindal, L.; Bruheim, P.; Klinkeberg, G.; Bredholt, H.; Nygard, G.; Doskeland, S. O.; Ellingsen, T. E.; Zotchev, S. B. *Chem. Biol.* **2009**, *16*, 1109.
- Takahashi, I.; Oda, Y.; Nishiie, Y.; Ochiai, K.; Mizukami, T. *J. Antibiot. (Tokyo)* **1997**, *50*, 186.
- Sugiyama, R.; Nishimura, S.; Kakeya, H. *Tetrahedron Lett.* **2013**, *54*, 1531.
- Morsy, N.; Houdai, T.; Konoki, K.; Matsumori, N.; Oishi, T.; Murata, M. *Bioorg. Med. Chem.* **2008**, *16*, 3084.
- Mouri, R.; Konoki, K.; Matsumori, N.; Oishi, T.; Murata, M. *Biochemistry* **2008**, *47*, 7807.
- Espiritu, R. A.; Matsumori, N.; Murata, M.; Nishimura, S.; Kakeya, H.; Matsunaga, S.; Yoshida, M. *Biochemistry* **2013**, *52*, 2410.
- Shui, G.; Guan, X. L.; Low, C. P.; Chua, G. H.; Goh, J. S.; Yang, H.; Wenk, M. R. *Mol. Biosyst.* **2010**, *6*, 1008.
- Feoktistova, A.; Magnelli, P.; Abeijon, C.; Perez, P.; Lester, R. L.; Dickson, R. C.; Gould, K. L. *Genetics* **2001**, *158*, 1397.
- Nishimura, S.; Arita, Y.; Honda, M.; Iwamoto, K.; Matsuyama, A.; Shirai, A.; Kawasaki, H.; Kakeya, H.; Kobayashi, T.; Matsunaga, S.; Yoshida, M. *Nat. Chem. Biol.* **2010**, *6*, 519.
- Lingwood, D.; Simons, K. *Science* **2010**, *327*, 46.
- Liu, J.; Tang, X.; Wang, H.; Oliferenko, S.; Balasubramanian, M. *K. Mol. Biol. Cell* **2002**, *13*, 989.
- Kaulin, Y. A.; Takemoto, J. Y.; Schagina, L. V.; Ostroumov, O. S.; Wangsp, R.; Teeter, J. H.; Brand, J. G. *J. Bioenerg. Biomembr.* **2005**, *37*, 339.
- Chemical structures of heronamides imply that hydrophobic ring and tail are inserted into the lipid membranes, whereas hydroxyl groups are located in the shallow area of the membranes. The presence of hydroxyl groups might stabilize the position of heronamides probably by hydrogen bonding with lipid head groups, which can explain the difference of the potency of metabolites **1** and **2**. Alternatively, hydroxyl groups could accelerate membrane binding or insertion through unrevealed mechanisms.
- Simons, K.; Vaz, W. L. *Annu. Rev. Biophys. Biomol. Struct.* **2004**, *33*, 269.

Supplementary Information

**Structure and biological activity of 8-deoxyheronamide C
from a marine-derived *Streptomyces* sp.: heronamides target saturated
hydrocarbon chains in lipid membranes.**

Ryosuke Sugiyama,[†] Shinichi Nishimura,^{*,†} Nobuaki Matsumori,[‡] Yuta Tsunematsu^{†,§}
Akira Hattori,[†] Hideaki Kakeya^{*,†}

[†]Department of System Chemotherapy and Molecular Sciences, Division of
Bioinformatics and Chemical Genomics, Graduate School of Pharmaceutical Sciences,
Kyoto University, Sakyo-ku, Kyoto 606-8501, Japan

[‡]Department of Chemistry, Graduate School of Science, Osaka University, Toyonaka,
Osaka 560-0043, Japan

[§]Present address: Department of Pharmaceutical Sciences, University of Shizuoka,
Shizuoka 422-8526, Japan

*Shinichi Nishimura, nshin@pharm.kyoto-u.ac.jp
Hideaki Kakeya, scseigyo-hisyo@pharm.kyoto-u.ac.jp

Supplementary methods: page S2-S4

Supplementary figures: page S5-S23

Supplementary table: page S24

References for Supplementary Information: page S25

Supplementary methods

Chemical compounds. Heronamides were isolated as described below. Heronamide C diacetate was prepared as described previously¹. 1-Palmitoyl-2-oleoyl-sn-glycero-3-phosphocholine (POPC), 1,2-dioleoyl-sn-glycero-3-phosphocholine (DOPC), 1,2-dimyristoyl-sn-glycero-3-phosphocholine (DMPC), porcine brain sphingomyelin (SM) were purchased from Avanti Polar Lipids, Inc. SM used in this study contained *N*-stearoyl-D-erythro-sphingosylphosphorylcholine as the most major constituent, around 50%. Ergosterol was from Acros Organics, cholesterol was from Nacalai Tesque, and amphotericin B was from LKT Laboratories, Inc. Nystatin and calcofluor white were purchased from Sigma. TNM-A was from the laboratory stock.

Yeast strains. *S. pombe* strains used in this study are JY1 (*h*⁻), HM123 (*h*⁻ *leu1-32*), *erg* mutants (*h*⁻ *ura4-C190T leu1-32 erg2::ura4*⁺, *h*⁻ *ura4-C190T leu1-32 erg31::ura4-FOA*^R *erg32::ura4*⁺, *h*⁻ *ura4-C190T leu1-32 erg4::ura4*⁺, and *h*⁻ *ura4-C190T leu1-32 erg5::ura4*⁺)², KGY2550 (*h*⁻ *css1-2*)³, and KP165 (*h*⁻ *leu1-32 bgs1-i2*)⁴. Rho1 was overexpressed in HM123 cells using pREP vectors⁵.

Screening for membrane binders. We screened microbial broths for membrane binding molecules that exhibit selective growth inhibition; culture broths that preferentially inhibited growth of wild-type cells compared to Δ *erg2* or Δ *erg31* Δ *erg32* cells could contain membrane binders. Growth inhibition was tested as described previously⁶. Briefly, mid-log phase inoculum in YE5S medium was diluted to 0.0033 OD₅₉₅ and cells were exposed to broth extracts dissolved in DMSO (1% v/v) at 30 °C for 24 h. After incubation, the turbidity was measured at OD₅₉₅ using an EnVision-2103 Multilabel Plate Reader (PerkinElmer). Broths that exhibited less growth inhibition against *erg* mutant cells were re-evaluated for their selectivity. The culture broth of *Streptomyces* sp. that contained heronamides was one of the hit broths.

Isolation of heronamides. Heronamides were obtained from the mycelium of *Streptomyces* sp.⁷ Mycelium collected from a 5 l culture was extracted with MeOH. The MeOH extract (3.0 g) was concentrated and partitioned between 60% MeOH and CHCl₃. The CHCl₃ layer (1.2 g) was fractionated by SiO₂ column chromatography (CHCl₃/MeOH), followed by ODS flash column chromatography (H₂O/MeOH). Fractions containing 8-deoxyheronamide C (83 mg) were subjected to RP-HPLC (Cosmosil-5C₈-MS) to give 14.5 mg of 8-deoxyheronamide C. Heronamides C (16.1 mg) and A (11.6 mg) were also purified by RP-HPLC (Cosmosil-5C₈-MS) from other fractions. The physico-chemical properties including UV, NMR and MS data of heronamides A and C were comparable to those reported¹.

Structure elucidation of 8-deoxyheronamide C (1). The molecular formula of compound **1** was established as C₂₉H₄₁NO on the basis of HR-FABMS (*m/z* 434.3045 [M+H]⁺, Δ_{mmu} = -0.9) and NMR spectral data, which suggested that compound **1** was a deoxy congener of heronamide C (**2**). In fact, the ¹³C NMR spectra of compound **1** possessed only one oxymethine carbon signal. Detailed analysis of 2D NMR data including COSY, HMQC and HMBC spectra revealed the planer structure of compound **1** as 8-deoxyheronamide C as shown in **Figure 1**. The absolute stereochemistry of compound **1** was unambiguously determined as described in the main text and **Supplementary Figures 5, 6 and 7**. ¹H and ¹³C chemical shift values, and HMBC and NOESY correlations of compound **1** are summarized in **Supplementary Table 1**.

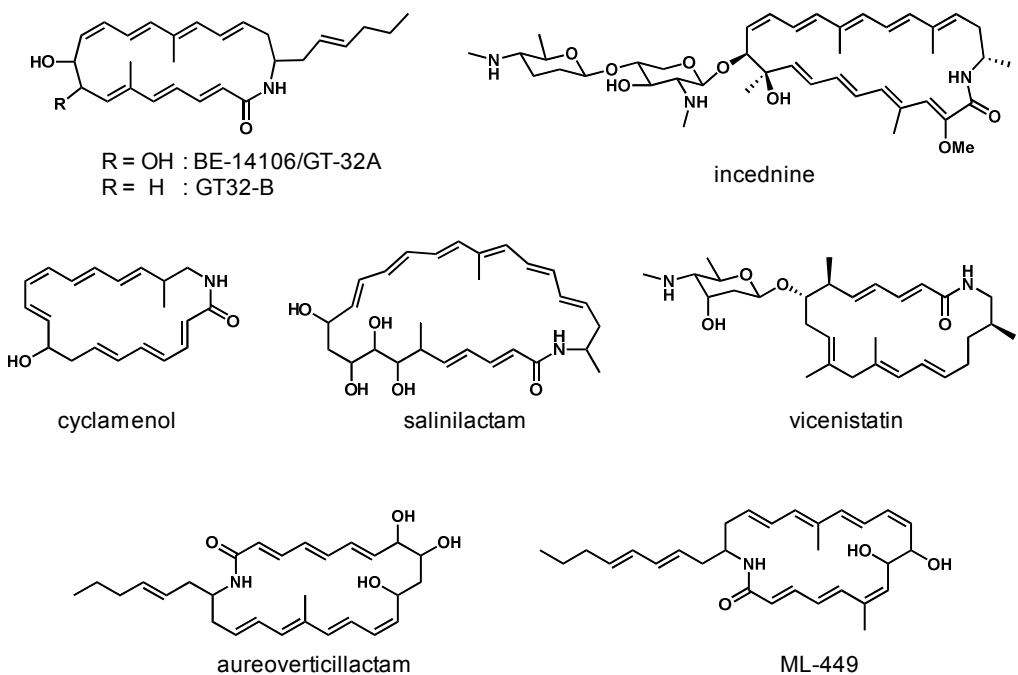
Preparation of liposomes for SPR analysis. Large unilamellar vesicles (LUVs) were prepared as described previously⁸. Phospholipid (POPC, DOPC, DMPC or SM) with or without 20 mol% sterol (ergosterol or cholesterol) were dissolved in chloroform in a round-bottom flask. The solvent was evaporated and the resulting lipid film was further dried *in vacuo* for over 2 hours. After hydrating with 1 mL of PBS buffer [10 mM phosphate buffer (pH 7.4), 2.7 mM potassium chloride, and 137 mM sodium chloride], the mixture was vortexed, sonicated, and subjected to three cycles of freezing (-80 °C), thawing (60 °C), and vortexing (5 s) to form multilamellar vesicles (MLVs). The MLV suspension was passed through double 100 nm polycarbonate filters 19 times with LiposoFast-Basic (AVESTIN Inc.) at room temperature to form LUVs. The LUVs were diluted with the same PBS buffer to produce a suspension with a final lipid concentration of 0.5 mM for injection into the SPR instrument.

Surface plasmon resonance experiments. 8-Deoxyheronamide C (**1**) (1.9 mg, 4.4 μmol), heronamide C (**2**) (3.2 mg, 7.1 μmol), heronamide A (**3**) (1.4 mg, 3.0 μmol) and heronamide C diacetate (**4**) (1.2 mg, 2.2 μmol) was dissolved in DMSO and stored as a 1 mM stock solution. 5 μL of the compound stock solutions were diluted to 50 μM with 95 μL of PBS buffer. This solution was further diluted with PBS buffer containing 5% DMSO to give 10 and 20 μM heronamide solutions. We ensured that all these solutions, together with the running buffer, had a same DMSO concentration. The SPR experiments were performed at 30 °C using a dodecylamine-modified CM3 sensor chip mounted on a Biacore T200 system (GE Healthcare), and the running buffer was PBS buffer containing 5% DMSO (pH 7.4). The unmodified CM3 sensor chip was first washed three times with a 50 mM NaOH/2-propanol solution [3:2 (v/v)] at a flow rate of 20 μL/min for 2 min. Dodecylamine was immobilized in one of the flow cells (fc2) of the CM3 chip with an amino coupling method while the other flow cell (fc1) was left untouched to serve as the control lane. The sensor chip was activated for 7 minutes by injecting a solution mixture (1:1 v/v, 70 μL) of 390 mM EDC and 100 mM NHS. Dodecylamine (1 mg/mL) in 10 mM acetate buffer containing 10% DMSO

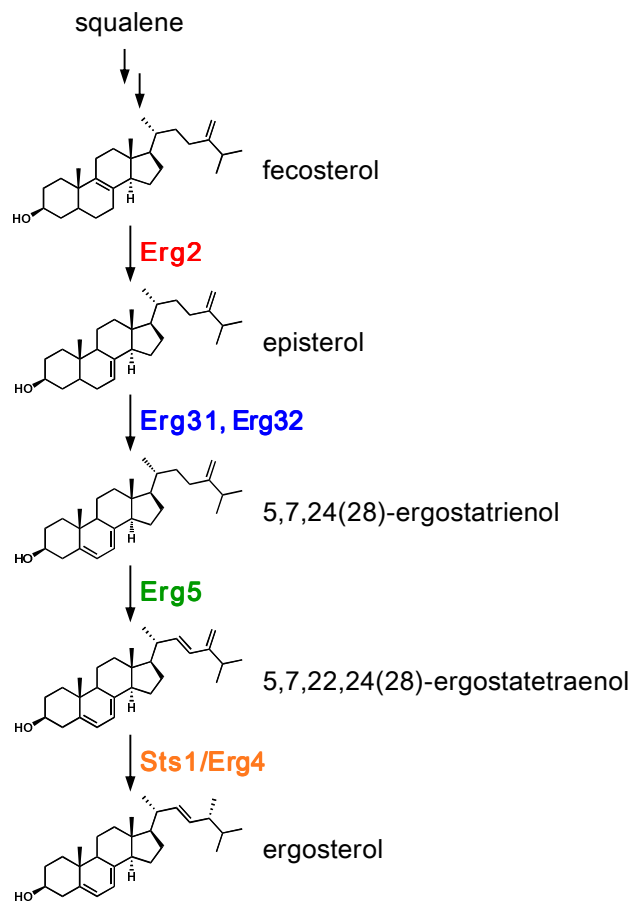
(pH 5.0, 35 μ L) was then injected for crosslinking. Remaining NHS ester groups on the sensor chip were deactivated by converting them to amide groups with an injection of 1 M ethanolamine hydrochloride (pH 8.5). The obtained modified sensor chip was washed with 10% DMSO to remove nonspecifically bound molecules. For the immobilization of liposomes on the sensor surface, the dodecylamine-modified sensor chip was first conditioned by an injection of running buffer at a rate of 10 μ L/min for 5 min. The liposome suspension (0.5 mM) was then injected at a flow rate of 2 μ L/min for 30 min, followed by the injection of 50 mM NaOH at a rate of 20 μ L/min for 2 min, three times to generate a stable sensorgram, which indicated the formation of a stable liposome layer on the sensor surface. Heronamide solutions, at a concentration of 10 or 20 μ M, were then injected at a flow rate of 10 μ L/min and the association was observed for 300 s. Then the running buffer was injected at the same flow rate for another 300 s, and the dissociation of heronamides from the surface was monitored.

Microscopy. For calcofluor white (Cfw) staining, cells were fixed with formalin, washed with PEM buffer (100 mM PIPES, pH 6.9, 1 mM EGTA, 1 mM MgSO₄), followed by resuspended in a Cfw solution of PEM buffer (0.5 μ g/mL). To collect images, we used a MetaMorph system (Universal Imaging Corp.) with an Olympus IX81 fluorescence microscope equipped with an UPLSAPO $\times 100$ lens.

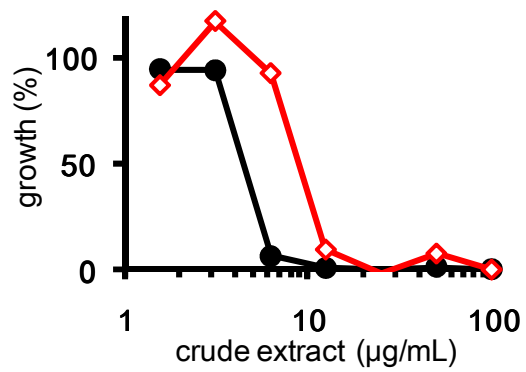
Supplementary Figures



Supplementary Figure 1. Chemical structures of polyene macrolactam metabolites.

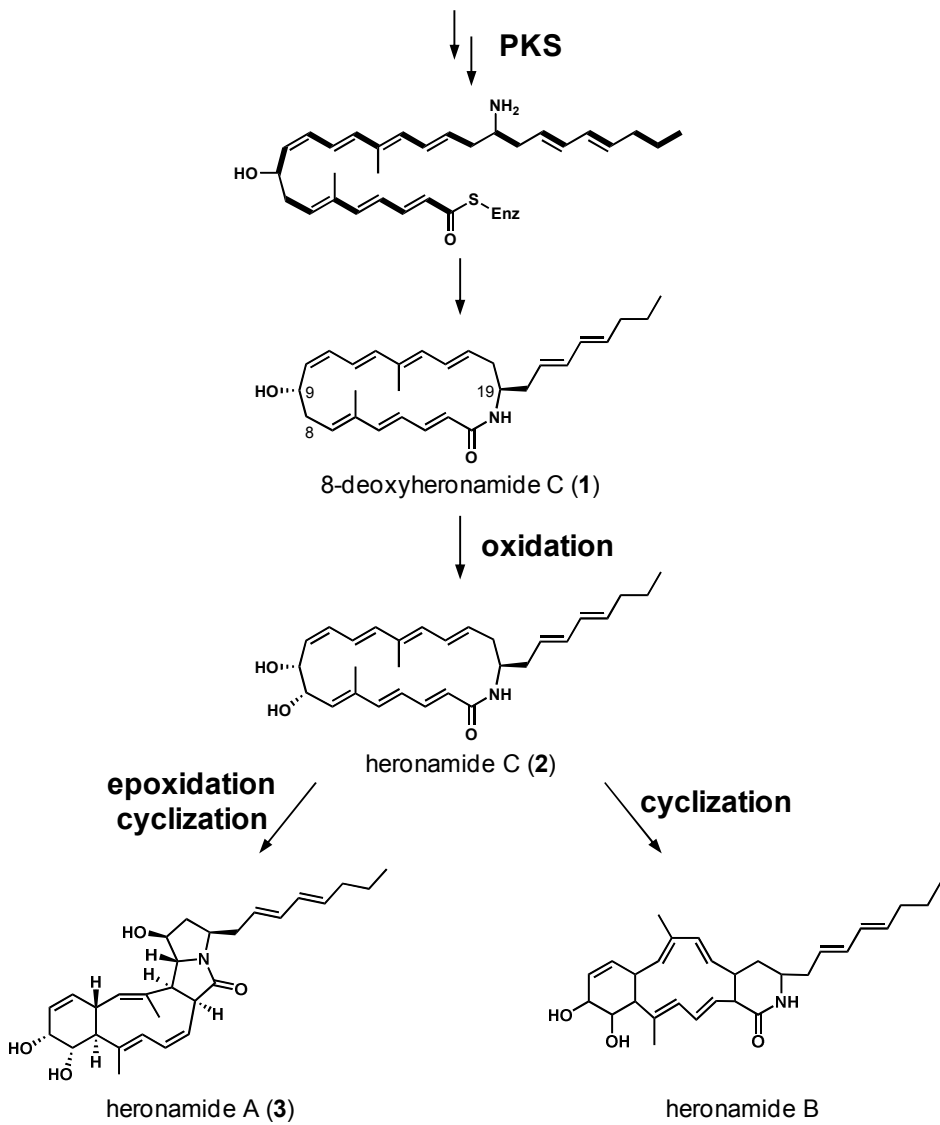


Supplementary Figure 2. Biosynthetic pathway of ergosterol in fission yeast².

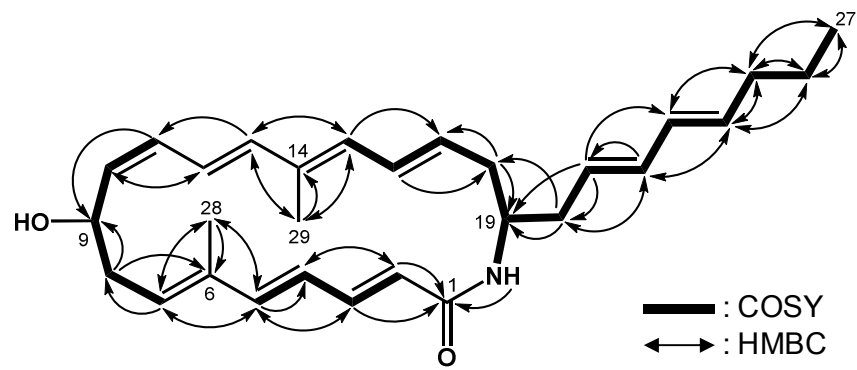


Supplementary Figure 3. Growth inhibitory activity of the culture extract of *Streptomyces* sp.

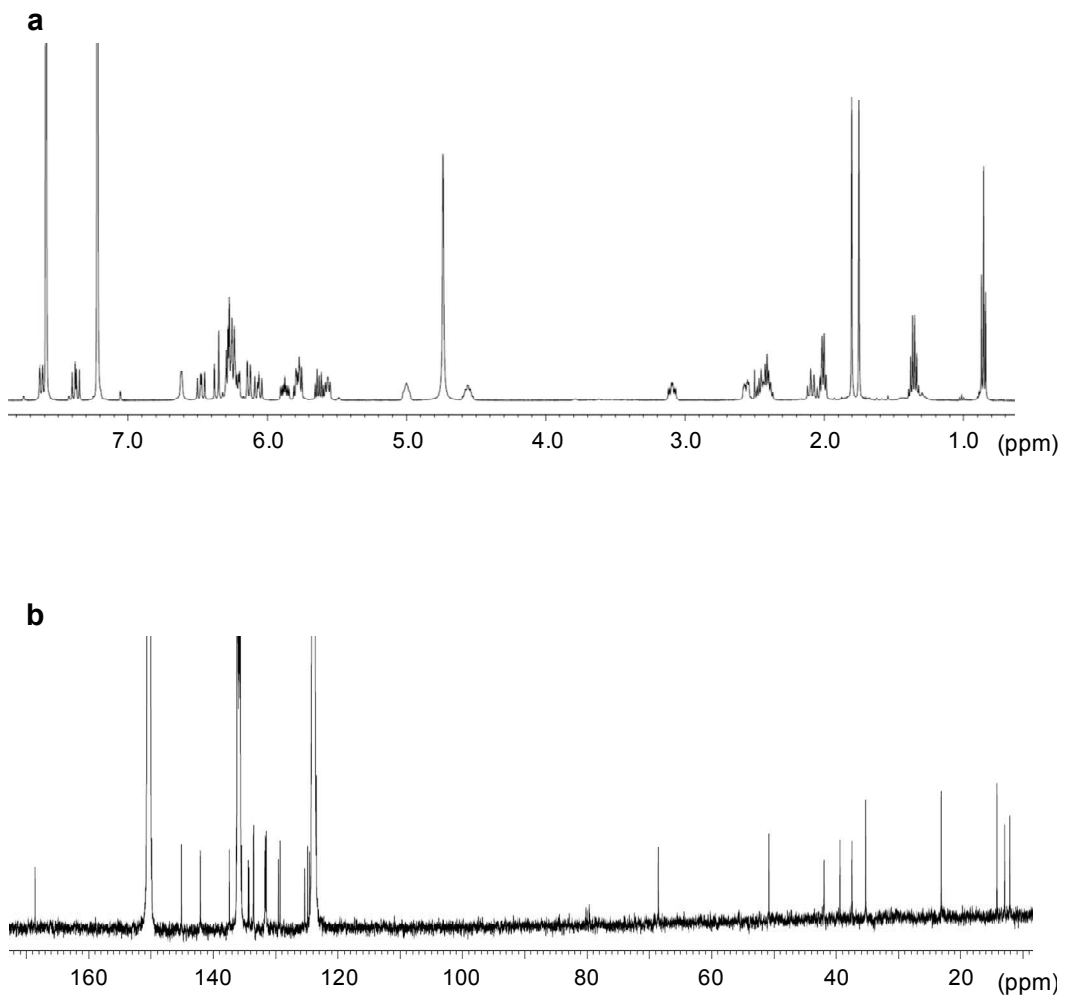
Growth curves of $\Delta erg2$ (red) and wild-type (black) cells are shown.



Supplementary Figure 4. Plausible model for the biosynthesis of heronamides. Based on the biosynthetic route of BE-14106 in *Streptomyces* sp. DSM 21069,⁹ it is expected that heronamide C (**2**) is produced by oxidation of 8-deoxyheronamide C (**1**) that is a PKS product. Heronamide A (**3**) is proposed to be produced from heronamide C (**2**) through epoxidation and tandem electrocyclic ring opening, whereas heronamide B is produced by cyclization of heronamide C (**2**).¹ This model suggests that heronamides should share the absolute configurations at C8, C9 and C19.

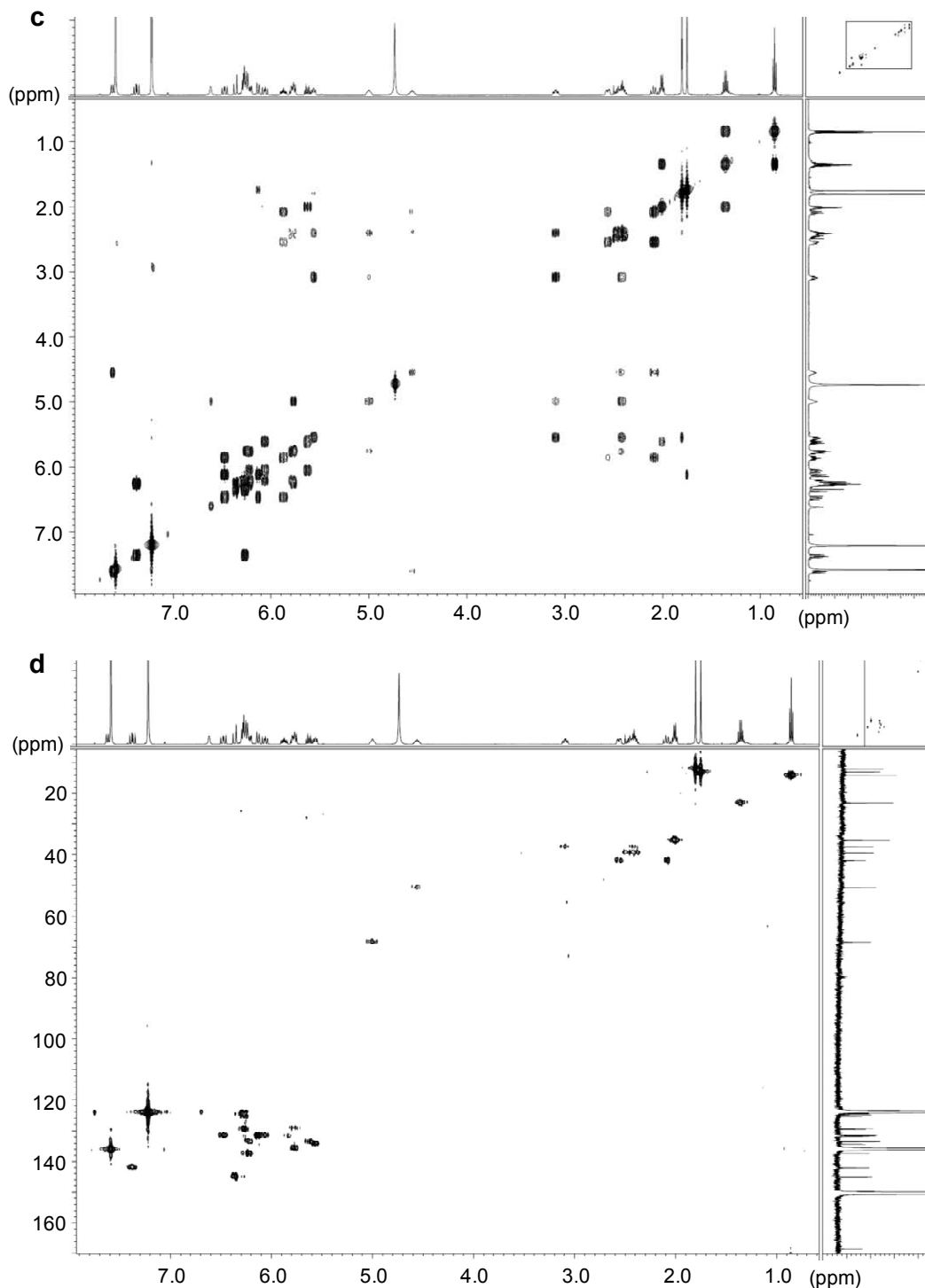


Supplementary Figure 5. Planar structure of 8-deoxyheronamide C (1). COSY and HMBC correlations are shown.



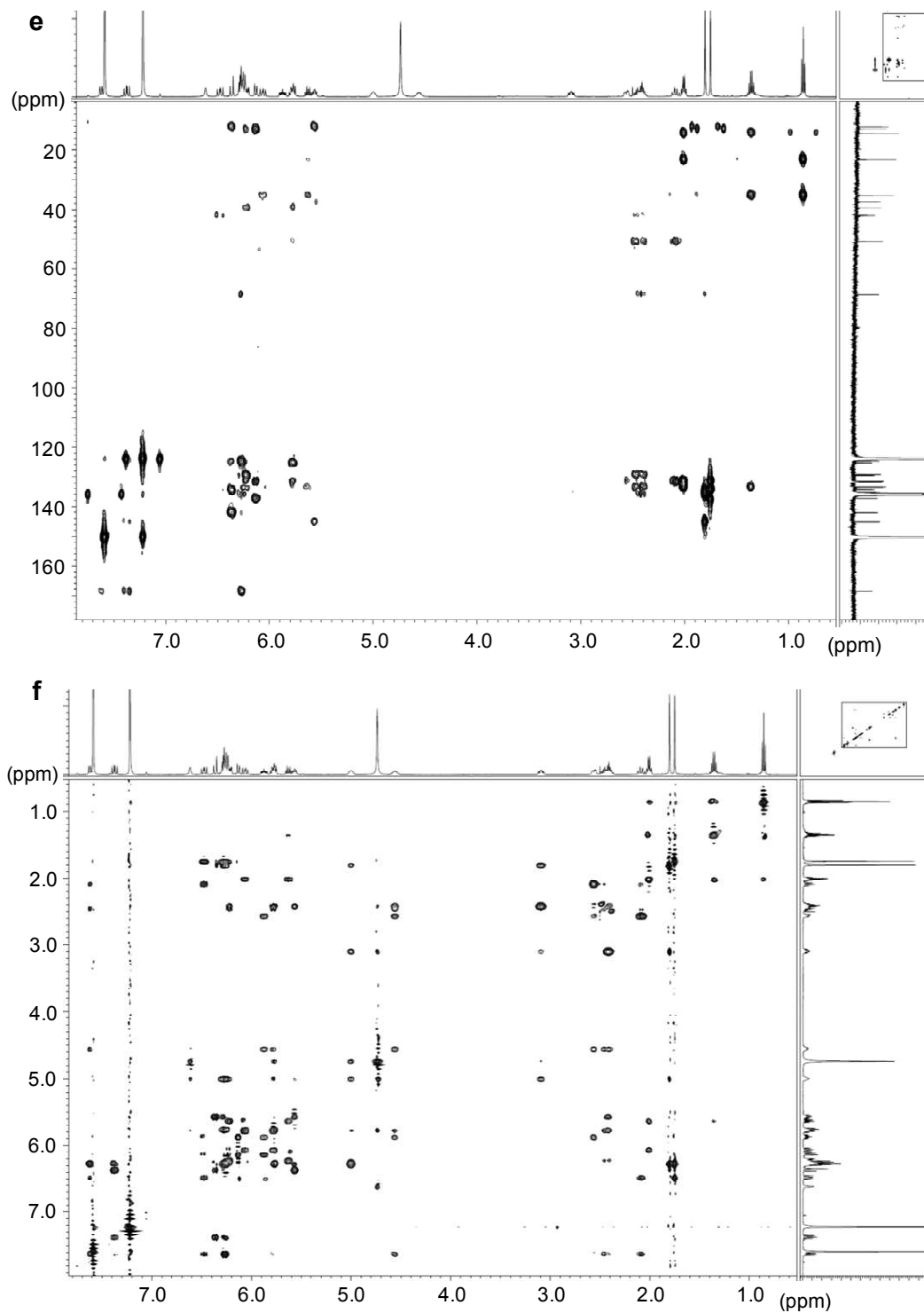
Supplementary Figure 6. NMR spectra of 8-deoxyheronamide C (1).

(a) ¹H NMR spectrum in pyridine-*d*₅ at 40 °C (500 MHz). (b) ¹³C NMR spectrum in pyridine-*d*₅ at 40 °C (125 MHz).



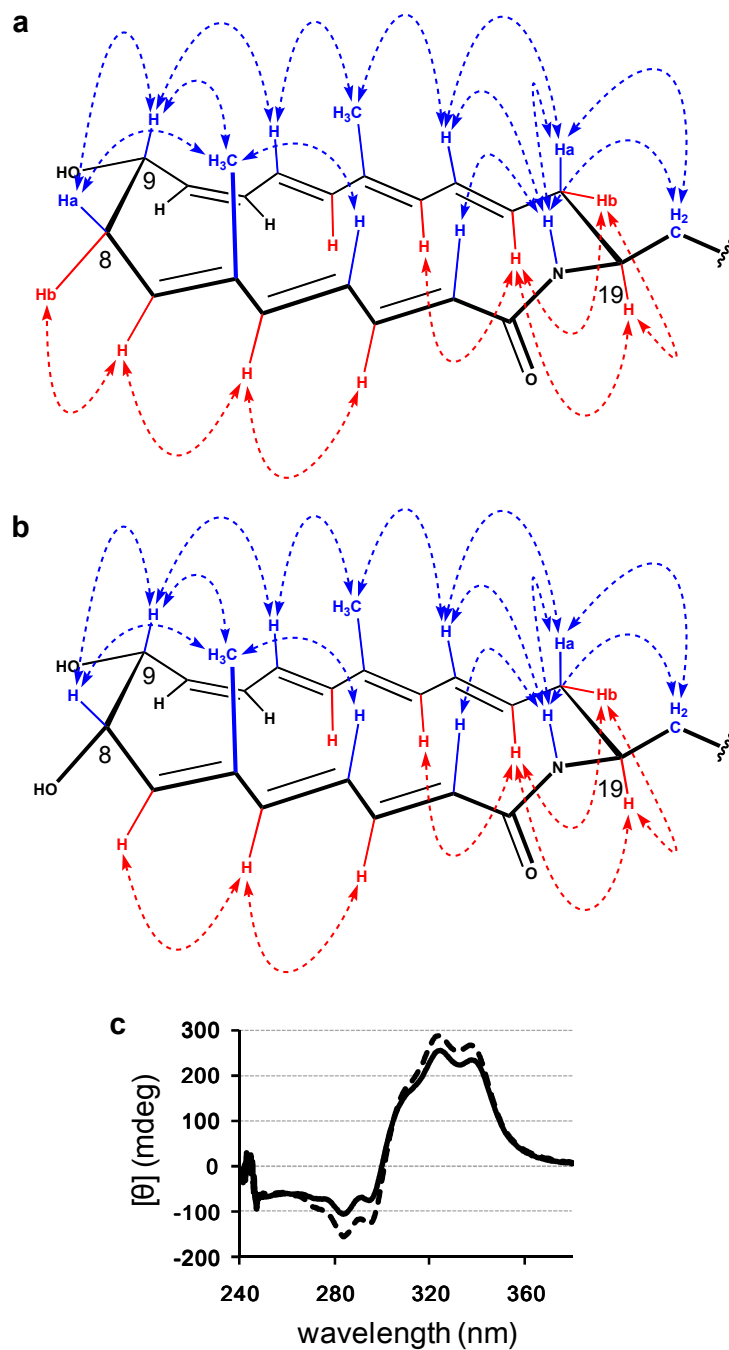
Supplementary Figure 6. NMR spectra of 8-deoxyheronamide C (1).

(c) COSY spectrum in pyridine-*d*₅ at 40 °C. (d) HMQC spectrum in pyridine-*d*₅ at 40 °C.

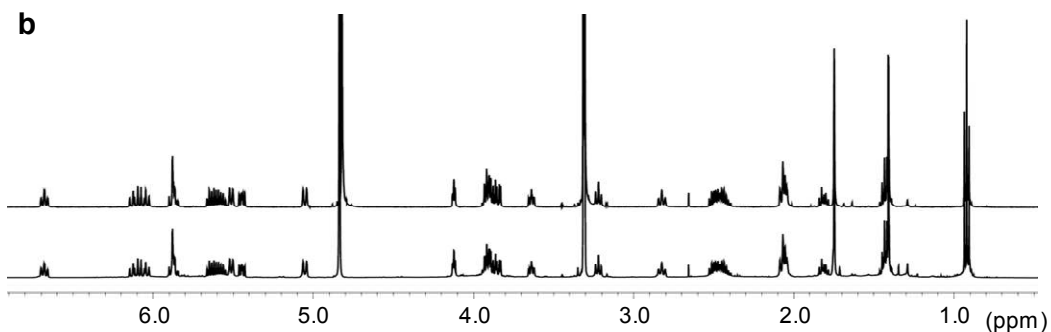
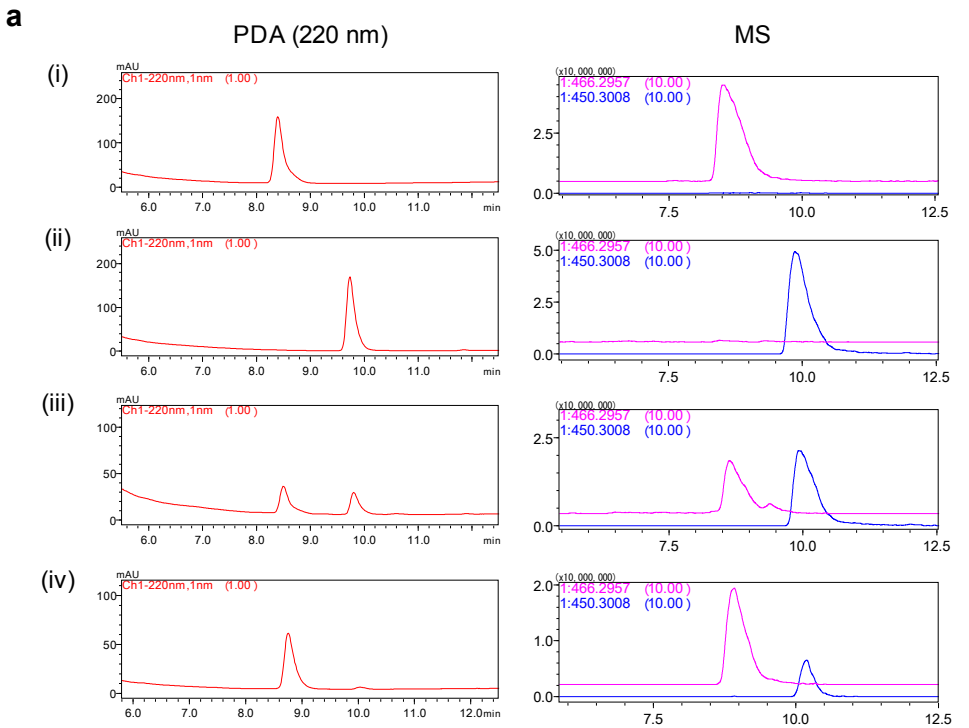


Supplementary Figure 6. NMR spectra of 8-deoxyheronamide C (1).

(e) HMBC spectrum in pyridine-*d*₅ at 40 °C. (f) NOESY spectrum in pyridine-*d*₅ at 40 °C.

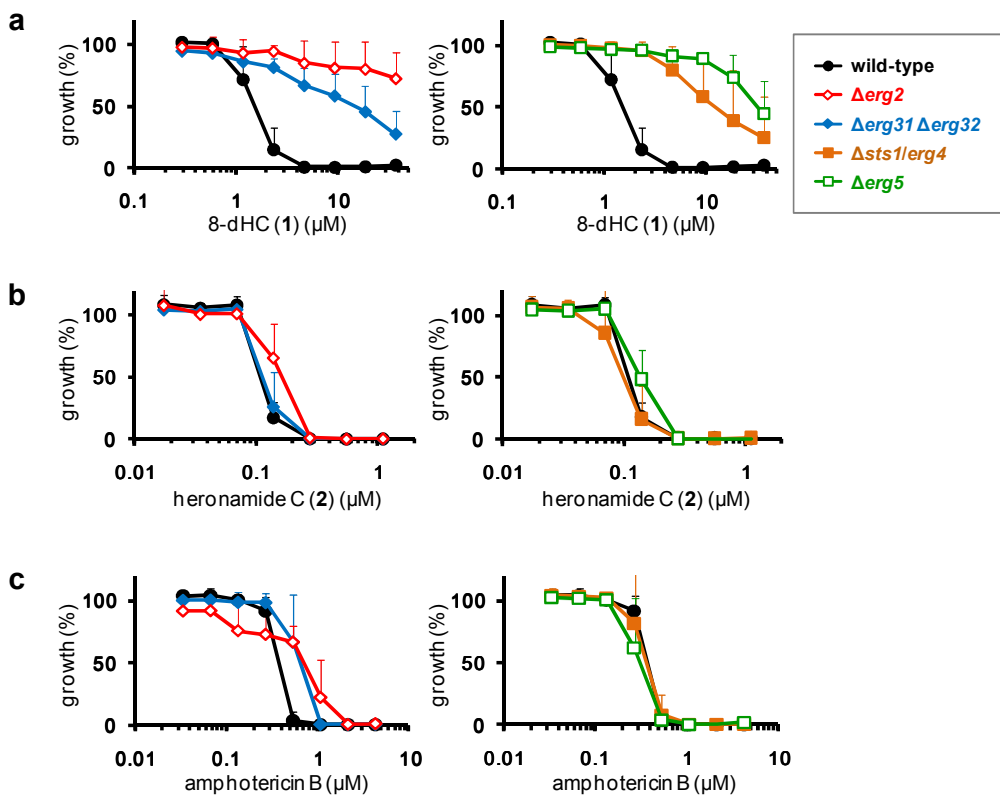


Supplementary Figure 7. Absolute stereochemistry of 8-deoxyheronamide C (1) and heronamide C (2). (a) Key NOESY correlations of 8-deoxyheronamide C (1). (b) Key NOESY correlations of heronamide C (2). (c) CD spectra of 8-deoxyheronamide C (1, solid line) and heronamide C (2, dashed line), measured in DMSO at a concentration of 100 μ M.

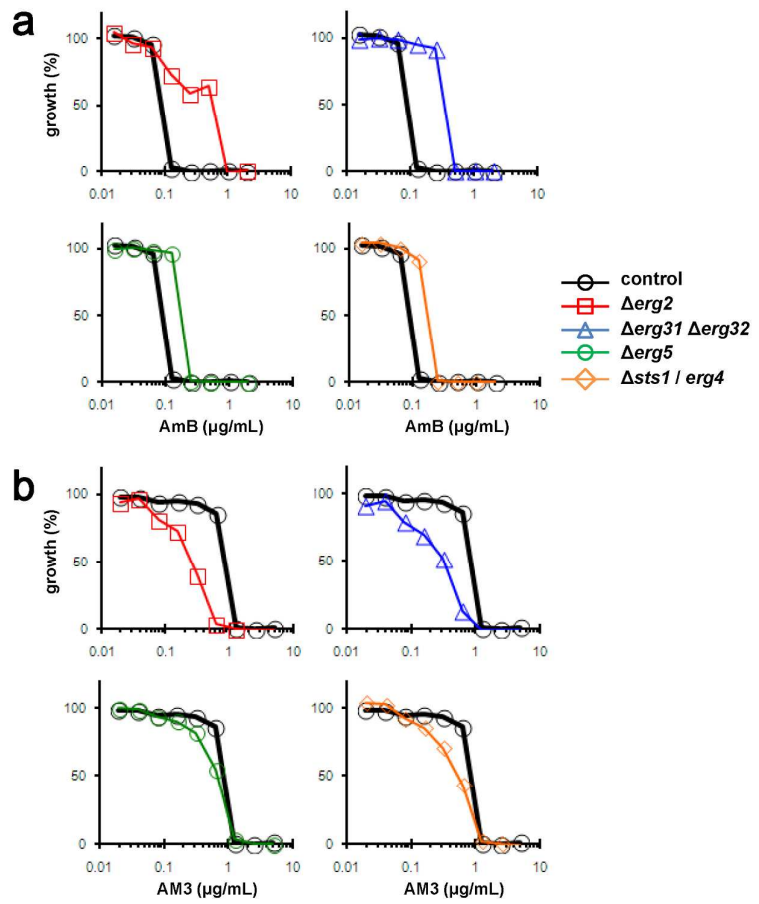


Supplementary Figure 8. Spontaneous conversion of heronamide C (2) to heronamide A (3).

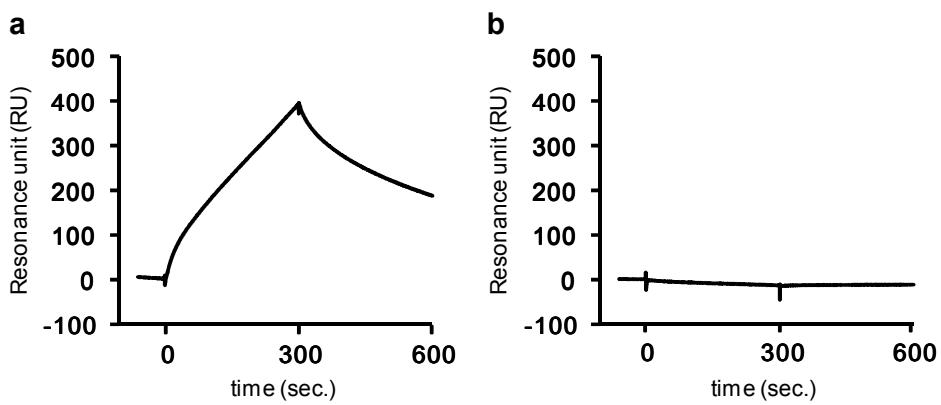
(a) LC-MS analysis of heronamides. Heronamide C (2) was dissolved in DMSO at a concentration of 0.5 mM and stirred at room temperature for 10 days. PDA (left) and MS (right) chromatograms for heronamide A (3) (i), heronamide C (2) (ii), a stirred solution of heronamide C (2) (iii), and co-injection of heronamide A (3) and the stirred solution of heronamide C (2) (iv) are shown. **(b)** ^1H NMR spectra of heronamide A (3) in methanol- d_4 . Heronamide A (3) isolated from the stirred solution of heronamide C (2) (upper) and heronamide A (3) isolated from the mycelium (lower) are shown. This unexpected conversion requires oxidation, S_N2 reaction, and cyclization as proposed.¹ Polyene compounds are known to be air-oxidized to furnish epoxide derivatives, although further reaction has not been mentioned.¹⁰ Precise mechanism for the reaction is under investigation.



Supplementary Figure 9. Effect of heronamides and amphotericin B on the growth of wild-type and *erg* mutant cells. Growth curves of $\Delta\text{erg}2$ (red), $\Delta\text{erg}31\Delta\text{erg}32$ (blue), $\Delta\text{sts}1/\text{erg}4$ (orange), $\Delta\text{erg}5$ (green) and wild-type JY1 (black) cells treated with (a) 8-deoxyheronamide C (1, 8-dHC), (b) heronamide C (2) or (c) amphotericin B are shown. Data represent means of three independent experiments. Error bars, s.d.

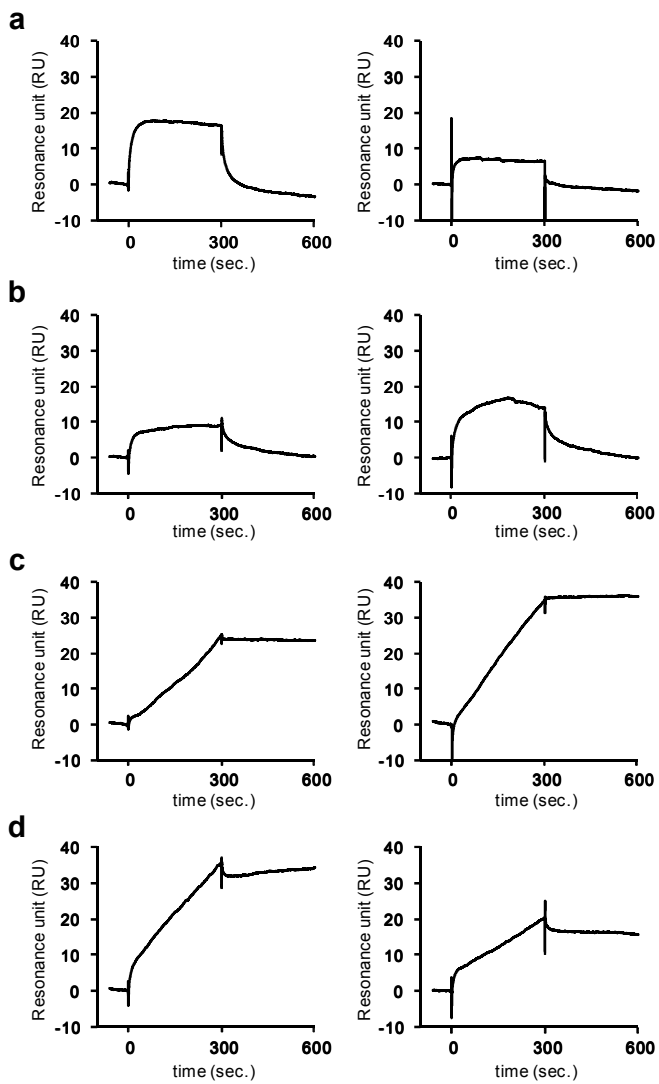


Supplementary Figure 10. Sensitivity of *erg* mutant cells to amphidinol 3. Cell growth inhibition by amphotericin B (AmB, **a**) and amphidinol 3 (AM3, **b**) was examined against *erg* mutant cells. The sensitivity profile was different between AM3 and AmB; none of *erg* mutant cells (colored line) were tolerant to amphidinol 3 compared to the control strain HM123 (black).

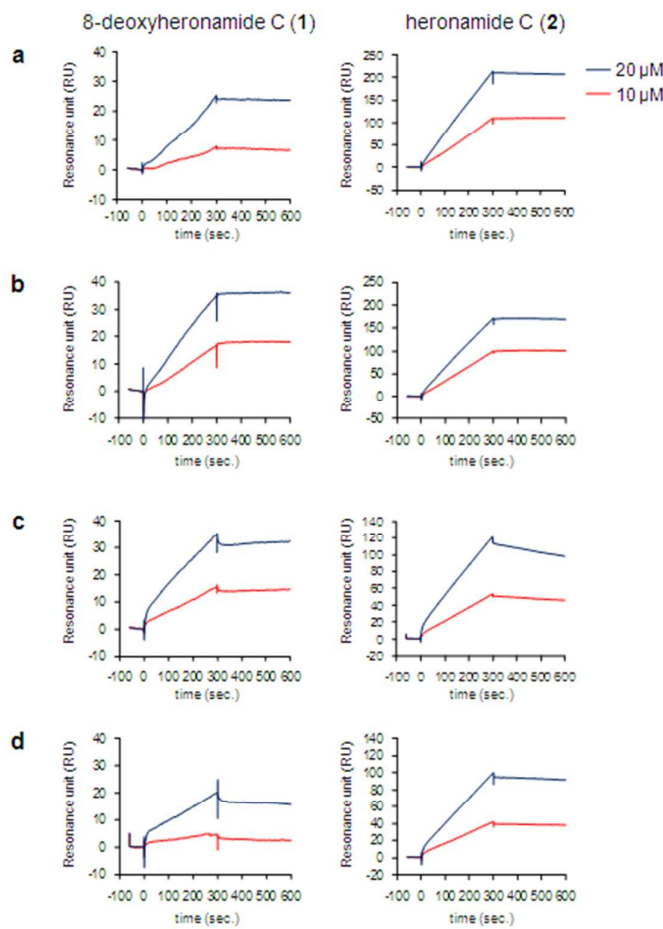


Supplementary Figure 11. Binding of amphotericin B to ergosterol-containing lipid membrane.

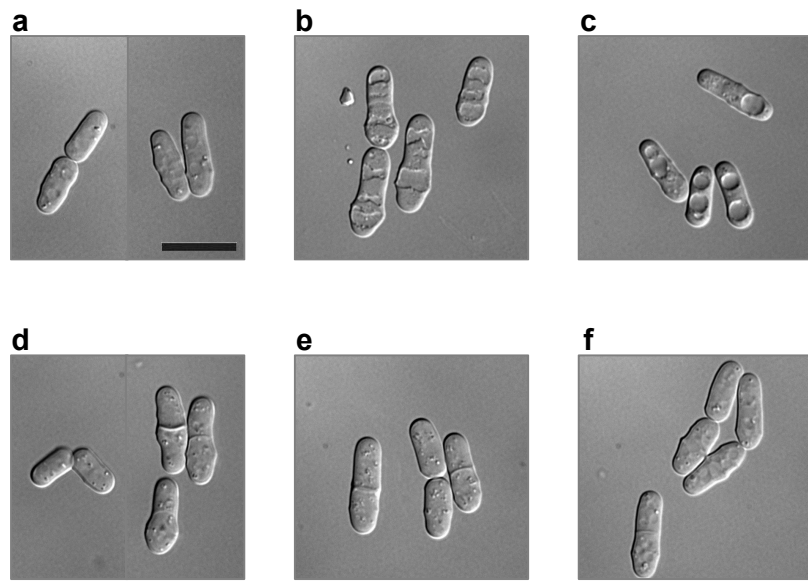
Liposomes consisting of POPC with (a) or without (b) 20 mol% ergosterol were immobilized on a dodecylamine-modified CM3 sensorchip. Elution of 20 μ M amphotericin B was started at time 0 and kept for 300 sec. The flow rate was 10 μ L/min.



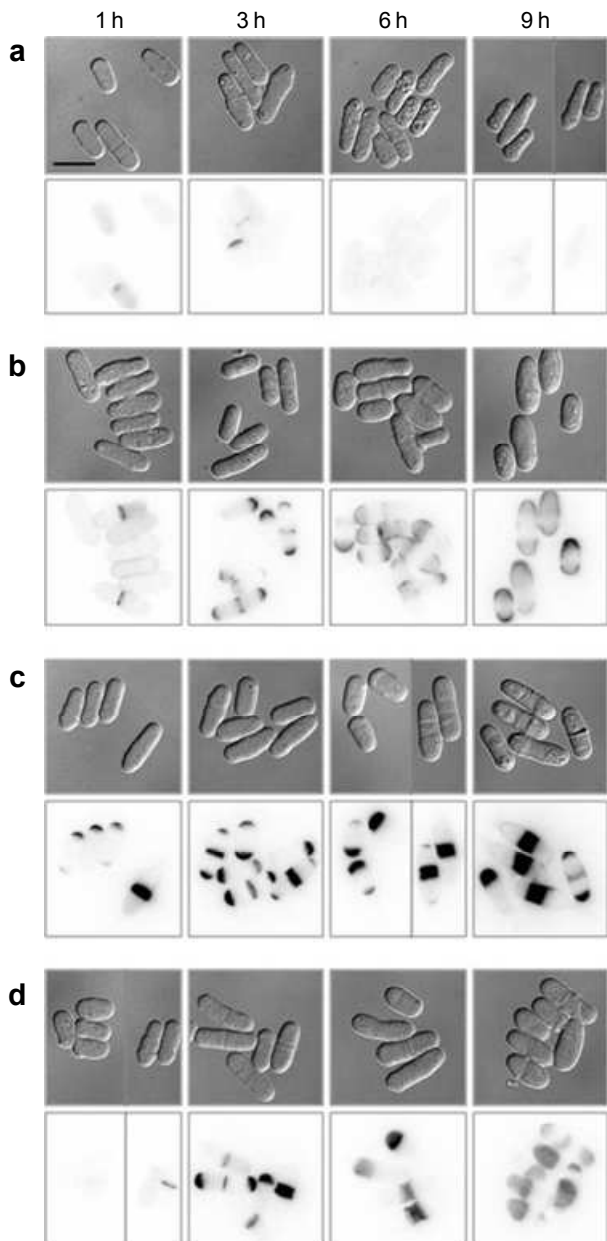
Supplementary Figure 12. SPR sensorgrams for binding of 8-deoxyheronamide C (1) to lipid membranes. DOPC (**a**), POPC (**b**), DMPC (**c**) or SM (**d**) liposomes with (left) or without (right) 20 mol% sterols (ergosterol in **a-c** and cholesterol in **d**) were captured on a dodecylamine-modified CM3 sensorchip. In this experiment, we used DMPC, not DPPC, both of which possess saturated acyl chains, because of the ease of treatment; the transition temperature of DMPC (~24 °C) is lower than DPPC (~43 °C). Experiments were conducted at 30 °C. Elution of 20 µM 8-dHC (**1**) was started at time 0 and kept for 300 sec. We could not test higher concentrations of 8-dHC (**1**) due to its low solubility. The flow rate was 10 µL/min.



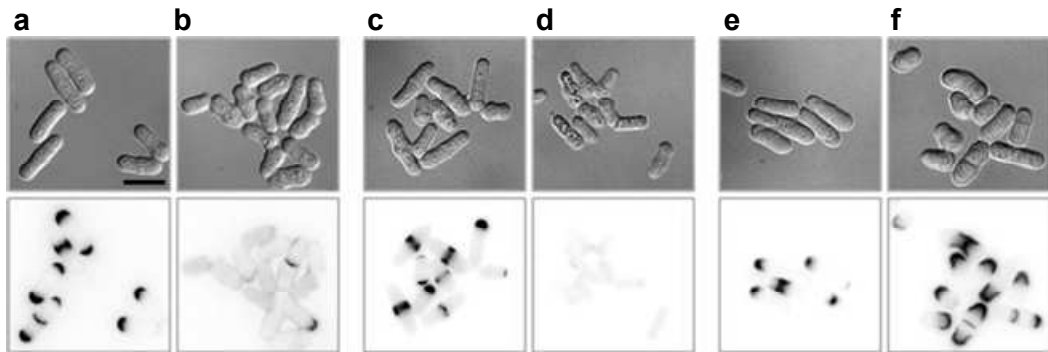
Supplementary Figure 13. SPR sensorgrams for binding of 8-deoxyheronamide C (1, left) and heronamide C (2, right) to lipid membranes. Liposomes made of DMPC with 20 mol% ergosterol (a), DMPC only (b), SM with 20 mol% cholesterol (c), or SM only (d) were captured on a dodecylamine-modified CM3 sensorchip. Concentration-dependent binding of analytes was observed. Experiments were conducted at 30 °C. Elution of 10 μM (red) or 20 μM (blue) of heronamides was started at time 0 and kept for 300 sec. The flow rate was 10 μL/min.



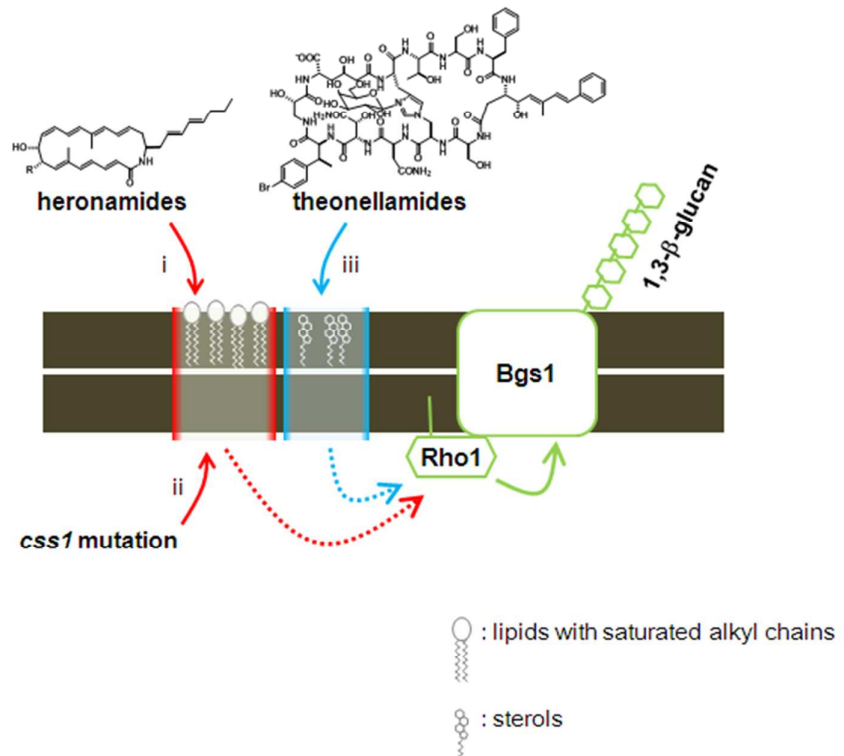
Supplementary Figure 14. Cell morphology after treatment with heronamides or polyene macrolide antifungals. Wild-type cells were treated with (a) DMSO (1% v/v), (b) amphotericin B (2 μ g/mL), (c) nystatin (5 μ g/mL), (d) 8-deoxyheronamide C (**1**) (20 μ M), (e) heronamide C (**2**), (2 μ M), or (f) heronamide A (**3**) (20 μ M), at 30 °C for 1 h. Scale bar, 10 μ m.



Supplementary Figure 15. Time course analysis of accumulation of cell wall material by chemical genetic or genetic perturbation. Wild-type cells were treated with (a) DMSO (1% v/v, solvent for compounds), (b) 8-deoxyheronamide C (**1**, 30 μ M), or (c) theonellamide A (1.1 μ M) at 30 °C. (d) Temperature-sensitive *css1* mutant cells were cultured at non-permissive temperature (37 °C). Cells were harvested after 1, 3, 6 or 9 h treatment, fixed, and stained with Cfw. Scale bars, 10 μ m. DIC (upper) and Cfw (lower) images are shown.



Supplementary Figure 16. Involvement of Bgs1 and Rho1 in the abnormal accumulation of cell wall material by 8-deoxyheronamide C (1). (a, b) Effect of *bgs1* mutation. Wild-type (a) or *bgs1* temperature-sensitive mutant cells (b) were incubated with 8-dHC (1) (10 μ M) at 27 °C for 2 h. The intense Cfw signals were not observed in *bgs1* mutant cells. (c-f) Effect of Rho1 overexpression. Cells transformed with empty vector (c) or pREP81-Rho1T20N (d) were grown at 30 °C for 16 h in EMM liquid medium and then challenged with 8-dHC (1) (10 μ M) for an additional 2 h. Effect of overexpression of Rho1 using pREP41-Rho1 (f) was also examined and compared with those of vector control (e). In all experiments, cells were fixed and stained with Cfw. Differential interference contrast (DIC, upper) and Cfw (lower) images are shown. Scale bar, 10 μ m.



Supplementary Figure 17. Model for the mechanisms of action of heronamides. Heronamides bind to lipids with saturated hydrocarbon chains, e.g. sphingolipids (i), while *css1* mutation changes sphingolipid species (ii). Theonellamides bind to 3 β -hydroxysterols (iii). Membrane domains colored in red, which is targeted by heronamides, might also be perturbed by *css1* mutation. In addition, membrane domains colored in blue, which is recognized by theonellamides, can be overlapped with those in red, since lipid raft domains consist of lipids with saturated alkyl chains and sterols. All three perturbations induce overproduction of cell wall material, which requires Rho1 and Bgs1 at least in the case of heronamides and theonellamides. How perturbation of membrane domain structures affect the functions of Rho1 and Bgs1 remains to be revealed (dotted lines).

Supplementary Table 1. NMR data of 8-deoxyheronamide C (1) in pyridine-*d*₅ at 40 °C

	¹ H (mult., <i>J</i> in Hz) ^{a,b}	¹³ C (mult.) ^{a,c}	HMBC	NOESY
1	-	168.6 (s)		
2	6.27 (m ^d)	124.5 (d)	C-1, C-4	NH
3	7.37 (dd, 10.6, 14.9)	142.1 (d)	C-1, C-5	H-5
4	6.26 (m ^d)	125.3 (d)	C-2	H ₃ -28
5	6.36 (d, 15.0)	145.1 (d)	C-3, C-4, C-7, C-28	H-3, H-7
6	-	135.6 (s)		
7	5.57 (br. dd)	134.4 (d)	C-5, C-8, C-28	H-5, H-8a
8a	2.41 (m ^e)	37.5 (t)	C-6, C-9	H-7, H-8b
8b	3.09 (ddd, 4.9, 10.0, 12.4)			H-8a, H-9, H ₃ -28
9	5.00 (m)	68.6 (d)		H-8b, H-12, H ₃ -28
9-OH	6.62 (br. s)	-		
10	5.78 (dd, 8.4, 10.7)	135.7 (d)	C-12	H-11
11	6.27 (m ^d)	129.6 (d)	C-9	H-10
12	6.26 (m ^d)	124.9 (d)	C-10	H-9, H ₃ -29
13	6.22 (d, 15.3)	137.4 (d)	C-11, C-15, C-29	
14	-	134.3 (s)		
15	6.13 (d, 11.3)	131.7 (d)	C-13, C-17, C-29	H-17
16	6.47 (dd, 11.3, 15.2)	131.5 (d)	C-18	H-18a, H ₃ -29, NH
17	5.87 (ddd, 5.3, 10.6, 15.2)	131.6 (d)		H-15, H-18b, H-19
18a	2.09 (m)	42.0 (t)	C-17, C-19	H-16, H-18b, NH
18b	2.56 (ddd, 2.6, 8.1, 12.8)			H-17, H-18a, H-19
19	4.56 (m)	50.8 (d)		H-17, H-18a, H ₂ -20, H-21, NH
20a	2.40 (m ^e)	39.4 (t)	C-18, C-19, C-22	H-19, H-21, H-22, NH
20b	2.46 (m ^e)			
21	5.78 (m)	129.3 (d)	C-19, C-20, C-23	H-19, H ₂ -20, H-23
22	6.23 (dd, 10.3, 15.1)	133.5 (d)	C-20, C-21, C-24	H ₂ -20, H-24
23	6.06 (dd, 10.3, 15.1)	131.5 (d)	C-25	H-21, H ₂ -25
24	5.63 (dt, 7.4, 15.1)	133.6 (d)	C-22, C-25, C-26	H-22, H ₂ -25, H ₂ -26
25	2.01 (dt, 7.4, 7.4)	35.3 (t)	C-23, C-24, C-26, C-27	H-23, H-24, H ₂ -26, H ₃ -27
26	1.36 (tq, 7.4, 7.4)	23.2 (t)	C-24, C-25, C-27	H-24, H ₂ -25, H ₃ -27
27	0.86 (t, 7.4)	14.2 (q)	C-25, C-26	H ₂ -25, H ₂ -26
28	1.80 (s)	12.1 (q)	C-5, C-6, C-7	H-4, H-8b, H-9
29	1.75 (s)	13.0 (q)	C-13, C-14, C-15	H-12, H-16
NH	7.62 (d, 10.3)	-	C-1	H-1, H-16, H-18a, H-19, H ₂ -20

^aChemical shift values were normalized using residual solvent peaks, δ_{H} 7.22 ppm and δ_{C} 123.9 ppm.

^b500 MHz.

^c125 MHz.

^{d,e}Signals overlapped.

References for Supplementary Information

- (1) Raju, R.; Piggott, A. M.; Conte, M. M.; Capon, R. J. *Org. Biomol. Chem.* **2010**, 8, 4682.
- (2) Iwaki, T.; Iefuji, H.; Hiraga, Y.; Hosomi, A.; Morita, T.; Giga-Hama, Y.; Takegawa, K. *Microbiology* **2008**, 154, 830.
- (3) Feoktistova, A.; Magnelli, P.; Abeijon, C.; Perez, P.; Lester, R. L.; Dickson, R. C.; Gould, K. L. *Genetics* **2001**, 158, 1397.
- (4) Deng, L.; Sugiura, R.; Ohta, K.; Tada, K.; Suzuki, M.; Hirata, M.; Nakamura, S.; Shuntoh, H.; Kuno, T. *J. Biol. Chem.* **2005**, 280, 27561.
- (5) Nakano, K.; Arai, R.; Mabuchi, I. *Genes Cells* **1997**, 2, 679.
- (6) Nishimura, S.; Arita, Y.; Honda, M.; Iwamoto, K.; Matsuyama, A.; Shirai, A.; Kawasaki, H.; Kakeya, H.; Kobayashi, T.; Matsunaga, S.; Yoshida, M. *Nat. Chem. Biol.* **2010**, 6, 519.
- (7) Sugiyama, R.; Nishimura, S.; Kakeya, H. *Tetrahedron Lett.* **2013**, 54, 1531.
- (8) Espiritu, R. A.; Matsumori, N.; Murata, M.; Nishimura, S.; Kakeya, H.; Matsunaga, S.; Yoshida, M. *Biochemistry* **2013**, 52, 2410.
- (9) Jorgensen, H.; Degnes, K. F.; Sletta, H.; Fjaervik, E.; Dikiy, A.; Herfindal, L.; Bruheim, P.; Klinkenberg, G.; Bredholt, H.; Nygard, G.; Doskeland, S. O.; Ellingsen, T. E.; Zotchev, S. B. *Chem. Biol.* **2009**, 16, 1109.
- (10) Rickards, R. W.; Smith, R. M.; Golding, B. T. *J. Antibiot. (Tokyo)* **1970**, 23, 603.